Partitioning protein ParP directly links chemotaxis to biofilm dispersal in *Pseudomonas aeruginosa*.

Jesse M. Reinhardt and Sonia L. Bardy[#]

Department of Biological Sciences, University of Wisconsin-Milwaukee, Milwaukee Wisconsin USA

Running Head: ParP directly links chemotaxis and biofilm dispersal

#address correspondence to: Sonia L. Bardy, bardy@uwm.edu.

Abstract

The recent characterization of partitioning proteins in the localization of chemotaxis signal transduction systems was proposed to have broad implications for polarly-flagellated non-enterobacteriaceae gamma-proteobacteria. These studies showed that the loss of either partitioning protein resulted in equivalent reductions in swimming motility and chemotaxis protein localization and inheritance. However, the role of these chemotaxis partitioning proteins outside of *Vibrio spp.* remains untested. Our studies on the chemotaxis partitioning proteins in *Pseudomonas aeruginosa* revealed an unexpected role for the partitioning protein ParP. While the *P. aeruginosa* ParC and ParP homologs are needed for wild type swimming motility, the loss of ParP results in a greater swimming defect compared to the *parC* mutant. Our studies revealed that the Par-like proteins directly interact with each other and the chemotaxis system, and ParP interacts with DipA. Deletion of *dipA* results in a similar defect in swimming motility as the *parP* mutant. ParP has an interdependence for polar cluster formation, but not localization, with both CheA and DipA, and CheA cluster formation is partially dependent on ParP. Due to the direct interactions and interdependence of cluster formation of ParP and DipA, and the similar phenotypes of the *parP* and *dipA* mutants, further investigation into the role of ParP in biofilm dispersion is warranted.

Importance

Impaired chemotaxis protein cluster formation or inheritance reduces chemotaxis which can have an impact on of the virulence of a bacterium. In some gamma-proteobacteria there are systems in place to ensure that chemotaxis proteins, like chromosomes and plasmids, are localized for optimal chemotaxis and that daughter cells inherit their own clusters for use after cell division. Par-like proteins have been implicated in the partitioning and localization of

chemotaxis proteins and the chemotactic ability of *Vibrio spp.* and *Rhodobacter sphaeroides* [1-3].We propose that Par-like proteins can do more than localize chemotaxis proteins to the poles of the cells. In *P. aeruginosa*, they bring together other key proteins involved in regulating flagellar-based motility, and we propose they function as a critical link between biofilm dispersal and motility.

Introduction

Spatial organization within bacterial cells results in the arrangement of proteins in distinct subcellular locations. This organization is not always static, and in some instances, can change in response to external cues or different stages within the bacterial lifecycle [4, 5]. There are a significant number of cellular processes that are affected by spatial organization and polarity, including signal transduction and motility. Bacterial chemotaxis is mediated by a two-component chemosensory system wherein a motile bacterium senses chemo-effectors in its environment and responds by moving towards favorable or away from unfavorable conditions. This system is best-studied in *Escherichia coli* where upon ligand binding, transmembrane methyl-accepting chemotaxis proteins (MCPs) will transduce the signal across the cytoplasmic membrane to the chemotaxis histidine kinase, CheA. CheA and the scaffolding protein CheW interact with the signaling domain of the MCP. The activation of CheA results in trans-autophosphorylation and transfer of the phosphate group to the response regulators CheY or CheB [6]. Phosphorylated CheY diffuses to the flagellar motor to cause a change in flagellar rotation, which results in a random change in swimming direction [7].

Specific localization patterns are known to be critical for optimal signal transduction [1, 8]. In *Vibrio cholera*, a polarly-flagellated gamma-proteobacterium, polar chemotaxis protein clusters are required for chemotaxis [1]. The Par-like proteins are required for proper cluster

formation and localization of the polar chemotaxis proteins [1, 2]. ParC and ParP are homologous to ParA and ParB, which are partitioning (Par) proteins that are used for partitioning plasmids and chromosomes upon cell division. Deletion of the Par-like proteins of *V. cholerae* altered flagellar rotation, swimming motility, and chemotaxis protein localization [1, 2]. Specifically, deletion of *parC* or *parP* from *Vibrio parahaemolyticus* resulted in a ~25-30% decrease in swimming motility and ~50-60% of cells either having aberrant chemotaxis protein localization or partitioning [2]. The Par proteins mark the old pole and are recruited through the diffusion and capture of ParC by a HubP-dependent anchor. ParP interacts with both MCPs and CheA, thereby stimulating array formation [9]. These chemotaxis partitioning proteins are conserved in all polarly-flagellated gamma-proteobacteria [1].

Pseudomonas aeruginosa, another Gram-negative polarly-flagellated gamma-proteobacterium, is ubiquitous in the environment and commonly found in water, soil and on man-made structures [10]. It can act as an opportunistic pathogen and significantly contributes to morbidity and mortality in chronic infections in Cystic Fibrosis patients [11]. In *P. aeruginosa*, the chemotaxis system controlling swimming motility is encoded in two gene clusters, cluster I (*che I*) and cluster V, and the encoded proteins localize to the poles [12, 13]. Within *che I* are genes encoding for ParC and ParP homologs that may have importance in swimming motility and chemotaxis protein localization.

Spatial organization in *P. aeruginosa* is driven through a polar determinant called the polar organelle coordinator, or POC, complex for the flagellum, type IV pili, and chemotaxis proteins [14]. The POC complex consists of three proteins: TonB3, PocA, and PocB, which are currently known to sit at the top of the flagellar localization hierarchy above FlhF [14]. In *tonB3*, *pocA*, and *pocB* mutants, FlhF, CheA, and the flagellum are mislocalized from the cell pole.

After the POC complex, FlhF is above all other known proteins for polar flagellar localization [15, 16]. Deletion of *flhF* results in mislocalized chemotaxis proteins and flagella, and reduced swimming motility [14]. Aside from FlhF and the Poc complex, there are no other major polar determinants of the chemotaxis system proteins known in *P. aeruginosa*.

Motility of *P. aeruginosa* is also affected by levels of bis-(3'→5')-cyclic dimeric guanosine monophosphate (c-di-GMP), a bacterial second messenger that also regulates biofilm formation and dispersion, differentiation, and virulence [17, 18]. In regards to chemotaxis and biofilm formation, c-di-GMP levels are widely known to dictate the switch between motile (planktonic) and sessile (biofilm) states of growth. While there are obvious benefits to growing in a biofilm, bacterial cells can revert to planktonic growth. Environmental signals such as glutamate or succinate trigger *P. aeruginosa* to switch from a biofilm to a planktonic mode of growth – this process is known as biofilm dispersion. Biofilm dispersion requires DipA, a c-di-GMP phosphodiesterase, to mediate a cellular reduction of c-di-GMP levels [18-20].

DipA is also involved in chemotaxis and its absence results in defects in swimming and swarming motility in bulk population assays [21]. *P. aeruginosa* exhibits individual cell c-di-GMP heterogeneity due to the asymmetrical inheritance of DipA [16]. Most *dipA* mutant cells have high levels of c-di-GMP, which results in an overall reduction in average cell velocity and flagellar reversals. DipA is polarly-localized and forms a complex with the flagellum and CheA. The localization of DipA is completely dependent on the presence of the chemotaxis histidine kinase CheA and the phosphorylation of CheA promotes DipA PDE activity [16].

In our studies, we determined what effect the loss of the Par-like proteins has on swimming motility and chemotaxis protein cluster formation and localization in *P. aeruginosa* PAO1. We performed a bacterial two-hybrid assay to identify proteins that interact with the Par-

like proteins. Finally, we examine the interdependence on cluster formation of the Par-like proteins with CheA and DipA. Our experiments suggest that the Par-like protein ParP is involved in the recruitment of the biofilm dispersal protein DipA to the flagellated pole.

Results

Par-like proteins are required for optimal chemotaxis in *Pseudomonas aeruginosa*. The chemotaxis gene cluster *che I* of *P. aeruginosa* encodes most of the genes required for chemotactic control of flagellar-based motility [13]. This includes the *par*-like genes *parC* and *parP* (Fig. 1A). Homologs of these genes are found in other polarly-flagellated non-Enterobacteriaceae γ-proteobacteria [2]. In *V. parahaemolyticus*, individual or double deletions of $parC_{Vp}$ and $parP_{Vp}$ resulted in a ~25-30% defect in swimming motility. This swimming defect was due to an increase in the percentage of the cell population that lack chemotaxis protein foci or have mislocalized (non-polar) chemotaxis protein foci [2]. Due to the amino acid sequence homology between ParC and ParP in *V. parahaemolyticus* and *P. aeruginosa* and the conserved genetic organization surrounding these genes, ParC and ParP were proposed to be important for swimming motility in *P. aeruginosa*. Deletion of *parC* and *parP* resulted in a 25% and 70% reduction in swimming motility, respectively, and could be partially complemented through expression of His-tagged fusion proteins (Fig. 1B). These results suggested that ParP has a more important role in chemotaxis than ParC. Negative controls for swimming motility and chemotaxis are provided by the *fliC::tn* mutant and cluster I mutant respectively. The *par*C and *parP* mutants have a similar growth rate as wild type, demonstrating that the swimming defect is not due to a growth defect (data not shown). Given that the swimming defect seen in the $parP_{Pa}$

mutants was significantly different from that reported in *Vibrio* [2], we further investigated the roles of these partitioning proteins in *P. aeruginosa*.

Chemotaxis protein localization is dependent on the Par-like proteins. To determine the cause of the swimming motility defects in the *parC*$_{Pa}$ and *parP*$_{Pa}$ mutants, we examined CheA (histidine kinase) localization and expression. The chemotaxis proteins of *P. aeruginosa* normally localize to the poles of the cell [22]. It has been previously demonstrated in *V. parahaemolyticus* that deletion of *parC*$_{Vp}$, *parP*$_{Vp}$, or both resulted in 50-60% of cells having a reduction in either chemotaxis protein foci formation or polar localization [2]. Through fluorescence microscopy, it was determined that in *P. aeruginosa* ParC and ParP were required for wild type levels of chemotaxis protein foci formation (Fig. 2). CheA-mTurquiose (CheA-mTq) expressed from the native site in the chromosome was used as a marker for chemotaxis protein foci formation and localization [16] as CheA, along with CheW and MCPs, are required for higher order clustering [23]. As a control, CheA foci formation was tested in the *cheW* mutant and showed a 96% reduction as previously published [22]. CheA foci formation was reduced by ~45-50% in the *parC*$_{Pa}$ and *parP*$_{Pa}$ deletion mutants (Fig. 2B). Surprisingly, in the *parC*$_{Pa}$ and *parP*$_{Pa}$ deletion strains, the localization of CheA foci remained largely unchanged compared to wild type. This suggests that the Par-like proteins are more important for foci stability or inheritance as opposed to localization in *P. aeruginosa*. The three amino acid residues that are different between CheA from PAO1 and PA14 do not affect function as the *P. aeruginosa* PAO1 strain expressing CheA-mTq from PA14 was capable of wild type chemotaxis (Fig. 2D) and therefore its use was justified for localization studies. The CheA-mTq fusion protein was present in all mutant backgrounds (Fig. 2B), demonstrating that the lack of foci formation was not due to reduced levels of CheA. Curiously, western blotting suggested that

148 CheA-mTq levels were slightly higher in the mutants compared to wild type (Fig. 2C). The
149 reason for this increase in CheA levels remains to be determined.

150 **DipA interacts with ParP$_{Pa}$ and affects swimming motility.** Because deletion of the *par*-like
151 genes affected swimming motility and chemotaxis protein foci formation in our work and in the
152 recent studies in *Vibrio spp*., we investigated protein interactions between ParC$_{Pa}$ and ParP$_{Pa}$ as
153 well as chemotaxis proteins and MCPs [1, 2, 9]. Given that the genome of *P. aeruginosa* is
154 reported to encode 23 MCPs that feed into the flagellar based chemotaxis system, a single
155 representative MCP (PA2867) was assayed for interaction with the Par-like proteins. A bacterial
156 two-hybrid (B2H) assay showed that ParC$_{Pa}$ and ParP$_{Pa}$ directly and strongly interact with each
157 other and weakly interact with CheA and the MCP (Fig. 3). ParC$_{Pa}$ could self-interact, thus
158 further suggesting that it is acting as a ParA-like protein [2, 24].

159 It was previously reported in *P. aeruginosa* strain PA14, that CheA co-
160 immunoprecipitated with the phosphodiesterase PA5017 (hereafter referred to as DipA for
161 clarity within the literature) [16]. This indicated that CheA and DipA form a complex with each
162 other, but it was not known if this interaction was direct or indirect. DipA is known to be
163 involved in biofilm dispersion and swimming motility and its ability to form polar foci and
164 degrade c-di-GMP is dependent on CheA [16, 18, 20]. Because the Par-like proteins affect
165 swimming motility and CheA foci formation, DipA and the Par proteins were assayed for direct
166 interactions to determine if the Par proteins aid in CheA/DipA complex formation. Strikingly, a
167 B2H assay revealed that ParP$_{Pa}$ directly and strongly interacts with DipA (Fig. 3). No direct
168 interaction could be detected between DipA and CheA or ParP and CheW using this assay.

169 In agreement with previous studies, the *dipA* mutant showed a 63% reduction in
170 swimming motility [16]. This was similar to the 70% reduction in swimming motility seen in the

171 *parP*$_{Pa}$ mutant, yet these results were significantly different from each other (Fig. 4A).
172 Complementation with His-DipA fully restored swimming motility to the *dipA* mutant (Fig. 4A).
173 A Western blot confirmed that His-DipA was expressed (Fig. 4B).

174 **DipA, ParP$_{Pa}$ and CheA polar localization is interdependent.** Given the similar phenotypes
175 and direct interaction between ParP and DipA, we investigated the localization dependence of
176 CheA, DipA and ParP$_{Pa}$ by fluorescence microscopy. CheA-mTq foci formation or localization
177 remained unchanged in a *dipA* mutant, indicating that CheA localization is independent of DipA
178 (Figs. 5A and B). Levels of CheA-mTq remained unchanged in the *dipA* mutant (Fig. 5C). Yfp-
179 ParP$_{Pa}$ foci formation was reduced by 50% in a *dipA* mutant and 60% in a *cheA* mutant, but there
180 was no change in localization (Fig. 6). DipA-Yfp foci formation was reduced by 50% in a *parP*$_{Pa}$
181 mutant and 95% in a *cheA* mutant (Fig. 7). The dependence of DipA on CheA for foci formation
182 has been previously published [16]. Expression of the ParP and DipA fluorescent fusion proteins
183 complemented the swimming defect of their respective mutant parent strains to the same levels
184 as the His-tagged ParP and DipA proteins (data not shown), thereby demonstrating that these
185 fusion proteins are as functional as the His-tagged versions. DipA was present at similar levels in
186 all mutant backgrounds, demonstrating that a loss of foci formation was not due to altered
187 protein levels (Fig. 7B). The levels of ParP fusion protein in the Δ*parP*Δ*cheA* and Δ*parP*Δ*dipA*
188 double deletion strains consistently appeared less than in Δ*parP*, suggesting ParP stability may
189 be affected by the loss of its interacting partners (Fig. 6B). Combined, the results of these
190 fluorescence microscopy studies on ParC, ParP, CheA and DipA localization show that there is
191 an interdependence on localization, particularly for ParP on CheA and DipA, DipA on ParP, and
192 CheA on ParP (Fig. 8).

193

Discussion

Chemotaxis proteins localize to distinct regions within a bacterial cell – this localization can vary depending on if it is a random or ordered process. A variety of mechanisms have been proposed including membrane curvature, stochastic nucleation, nuclear exclusion and interaction with the Tol-Pal complex [25-29]. These different mechanisms may not be exclusive of each other as these studies focus on different bacteria such as *E. coli* and *Bacillus subtilis*, as well as different MCPs within the same species. In *E. coli*, MCPs localize to the poles as large clusters, yet small clusters and individual proteins can be seen at the lateral regions of the inner membrane [26]. Other organisms, such as *Vibrio spp*. and *R. sphaeroides*, have *par*-like genes in their chemotaxis gene clusters and the encoded proteins are used for chemotaxis protein cluster formation and localization [1-3]. *P. aeruginosa* has *par*-like genes encoded in its main chemotaxis gene cluster, *che I* (Fig. 1A), and this work provides convincing evidence that these Par-like proteins are involved in chemotaxis and linked to DipA, a c-di-GMP phosphodiesterase involved in biofilm dispersion and motility regulation.

The Par-like proteins are known to be involved in swimming motility, chemotaxis and polar array formation in *Vibrio* spp. [1, 2, 9]. Our work shows that in *P. aeruginosa*, $ParC_{Pa}$ and $ParP_{Pa}$ are needed for optimal swimming motility (Fig. 1B). Comparison of the phenotypes between *V. parahaemolyticus* and *P. aeruginosa* reveal that the $parP_{Vp}$ mutant has a swimming defect equal to the *V. parahaemolyticus parC* mutant. However, $ParP_{Pa}$ is distinct in that it appears to have a more significant role in swimming motility, and possible reasons for this will be discussed below.

The Par-like proteins are known to dimerize and interact with each other and with the chemotaxis system via CheA and the MCPs in *V. parahaemolyticus* [2, 9]. Our work confirms

that ParC$_{Pa}$ can dimerize and strongly interact with ParP$_{Pa}$, and both proteins interact with CheA (Fig. 3). We did not observe ParP$_{Pa}$ self-interaction (data not shown). In agreement with earlier studies, it was determined that the Par-like proteins of *P. aeruginosa* interacted with a representative MCP, thus demonstrating that ParC$_{Pa}$ and ParP$_{Pa}$ are not linked to the chemotaxis system only via CheA [9]. Strikingly, we found that ParP$_{Pa}$ interacted strongly with DipA (Fig. 3). These results are novel, as ParP$_{Pa}$ and DipA form the first direct link between the biofilm dispersion and chemotaxis systems. It was previously shown by co-immunoprecipitation that DipA and CheA form a complex, but it was not known if this was through direct or indirect interactions [16]. Additionally, this earlier publication focused on the role of DipA (referred to as Pch) in motility and did not address the role of this phosphodiesterase in biofilm dispersal [16, 18].

The *dipA* mutant had a reduction in swimming motility that was similar, but significantly different to what was seen in the *parP$_{Pa}$* mutant (Fig. 4A). Localization studies suggest that the motility defect may be due to the loss of ParP as well as altered c-di-GMP levels at the cell pole. In *P. aeruginosa* PA14, Kulasekara *et al* [16] showed that loss of DipA leads to a loss of c-di-GMP heterogeneity in individual cells, with most cells having high levels of c-di-GMP. A reduction in flagellar reversals and average cell velocity compared with wild type was also observed. These results suggest that c-di-GMP levels modulate flagellar reversals and cell velocity, however, the mechanism by which this occurs has not been determined but may involve a c-di-GMP effector protein. DipA forms polar foci at the flagellated pole with CheA. After cell division, one of the daughter cells will inherit the flagellum and a DipA cluster, which lowers the c-di-GMP levels in that cell, thus creating c-di-GMP heterogeneity in individual cells. The role of this heterogeneity is speculated to give a survival advantage to these cells in unpredictable

environments [16]. Individual cells with high or low c-di-GMP levels would likely tend to either attach to a surface and start biofilm formation or remain motile and spread to new areas. In this sense, at any moment, there are cells that are "primed" for either choice, depending on the environment. The presence of CheA is absolutely required for DipA polar localization and the phosphorylation activity of CheA promotes DipA PDE activity. The GTPase FlhF is required for polar localization of the flagellum, and in an *flhF* mutant, the flagellum is still produced but mislocalized from the pole [30]. This results in cells having reduced swimming and swarming motility. Loss of FlhF also results in a reduction of transcription of class II, III or IV flagellar genes [30]. FlhF is above CheA and DipA in terms of dictating polar localization, but not their association with each other [16]. The absence of FlhF results in the mislocalization of the flagellum, and CheA and DipA foci from the pole. This suggests that the flagellum, CheA and DipA form a complex at one pole of the cell. However, it is not known if these three components remain in a complex when they are mislocalized from the pole. By forming these protein complexes, new daughter cells will be more likely to inherit necessary chemotaxis proteins to be used right away or once they synthesize a new flagellum.

Using fluorescence microscopy, we tested chemotaxis protein localization in the absence of the Par-like proteins. Deletion of either $ParC_{Pa}$, $ParP_{Pa}$ or CheW resulted in a loss of CheA cluster, or foci, formation, but not polar localization in *P. aeruginosa* (Fig. 2). Comparable results were seen for the Par-like proteins in *V. parahaemolyticus*, except that of the cells that had aberrant clustering, 50% of them had no clusters while the other 50% had non-polar clusters [2]. These results suggest that in *P. aeruginosa*, the Par-like proteins function more in cluster stability as opposed to localization, but we cannot rule out technical differences as the cause of this discrepancy. Our results for the loss of CheA cluster formation in a *cheW* mutant agree with

263 previously published work [22]. Interestingly, we show that the loss in CheA cluster formation
264 also coincided with a slight increase in CheA levels in the cells (Fig. 2C). The absolute levels of
265 MCP, CheW and CheA proteins can vary in a bacterium, but their stoichiometry appears to
266 remain constant [6, 31]. Overexpression of a chemotaxis protein can reduce chemotaxis and
267 cluster formation [31, 32]. One possible explanation for the reduction in CheA cluster formation
268 in *P. aeruginosa* is that excess levels of CheA are present in the cell relative to the MCP and
269 CheW proteins. However, our results do not show if the stoichiometry of MCP:CheW:CheA was
270 altered - this would require further investigation.

271 The Par-like proteins are interdependent in their polar cluster formation. $ParC_{Vp}$ and
272 $ParP_{Vp}$ are both needed for their cluster formation and polar localization in *V. parahaemolyticus*
273 [2]. While we have not tested the interdependence of $ParC_{Pa}$ and $ParP_{Pa}$, our work has shown that
274 the clustering ability of $ParP_{Pa}$ is interdependent on both CheA and DipA and that loss of cluster
275 formation is ~50% (Figs. 6 and 7). These results suggest that the interdependence of localization
276 between these proteins are equally important in their cluster formation. In a previous study and in
277 this work, DipA cluster formation requires CheA [16]. However, we found that CheA cluster
278 formation and cellular levels are not dependent on DipA (Fig. 5).

279 In summary, this work showed that the Par-like proteins of *P. aeruginosa* PAO1 are
280 involved in chemotaxis controlling swimming motility. Our results correlate well with other
281 studies in terms of the effects of the Par-like proteins on swimming motility and chemotaxis
282 protein foci formation. Notably, we found that $ParP_{Pa}$ plays a more significant role in swimming
283 motility than $ParC_{Pa}$. We discovered that the c-di-GMP phosphodiesterase DipA directly
284 interacts with $ParP_{Pa}$ and that they have an interdependence in their cluster formation. These
285 results suggest that $ParP_{Pa}$ and DipA work in the same pathway and this may be the mechanism

behind the large decrease in swimming motility in a *parP* mutant. We have provided compelling evidence that the chemotaxis and biofilm dispersion systems are linked together via DipA and $ParP_{Pa}$ (Fig. 8). When biofilm cells sense a nutrient cue to disperse, *dipA*, motility, and chemotaxis genes are upregulated, c-di-GMP levels decrease, the extracellular matrix is broken down, and cell adhesiveness is reduced [18, 20]. Due to this series of events, cells become motile and chemotactic, and leave the biofilm. This leads to the question of what role $ParP_{Pa}$ has in this process of dispersion and if DipA proteins can temporally, and perhaps spatially, switch between interactions with biofilm dispersal proteins and chemotaxis proteins, or if there are functionally separate pools of this protein within the cell. To our knowledge, the localization of DipA has not yet been determined in biofilm or biofilm-dispersed cells. Future studies will determine in more detail how the loss of $ParP_{Pa}$ has a greater defect in swimming motility than the loss of $ParC_{Pa}$ and if $ParP_{Pa}$ has a role in biofilm dispersion.

Materials and Methods

Strains, plasmids, growth conditions and media used. Lists of plasmids and strains used in this publication are in Supplemental Tables 1 and 2, respectively. All *P. aeruginosa* strains generated in the work are derived from *P. aeruginosa* PAO1 (Iglewski strain). Both *E. coli* and *P. aeruginosa* were grown in Lysogeny Broth (LB) with aeration and on LB 1.5% agar plates at 37°C. Antibiotics were used at the following concentrations as appropriate: 50 µg/mL of gentamycin and 70 µg/mL of tetracycline for *P. aeruginosa* and 15 µg/mL of gentamycin, 30 µg/mL of kanamycin, 25 µg/mL of chloramphenicol and 10 µg/mL of tetracycline for *E. coli*.

Generation of deletion mutants and expression strains. In-frame gene deletions of *cheA* and *parC* were generated by homologous recombination using the suicide vectors pEX18Tc or

pEX19Gm as previously described [33, 34]. Briefly, 1 Kb DNA fragments upstream and downstream of the genes of interest were PCR amplified and fused together through splicing by overlap extension (SOE) PCR using PAO1 DNA as template [35]. Primers are listed in Supplemental Table 3. Fusion constructs were sequenced to ensure no undesired mutations were introduced. This resultant fragment was cloned into pEX18Tc or pEX19Gm and transformed into *E. coli* S17-1 for mating into *P. aeruginosa* PAO1. Merodiploids were selected on tetracycline or gentamycin, as appropriate, with chloramphenicol [5 µg/mL] providing counter-selection against *E. coli*. Resolution of the merodiploids was achieved through 10% sucrose counter-selection, and the deletions were confirmed by PCR. Gene deletions of *cheW*, *dipA*, and *parP* were performed as above except the upstream and downstream 1 Kb DNA fragments included nine basepairs from the 5' and 3' ends of the target gene. This approach was used to reduce the likelihood of polar effects.

Incorporation of *cheA-mTq* into the native site of the chromosome was done using a *cheA-mTq*:pEX19Gm construct [16] as above. In this construct, *cheA* from *P. aeruginosa* PA14 was used. The CheA amino acid sequences from strains PAO1 and PA14 are 99.6% identical, with three residues [E133A, A161V and P191S, respectively] being different between them. The *dipA-yfp* fusion was amplified, sequenced, and cloned into pJN105 [16, 36]. The *yfp-parP* fusion was generated by SOE PCR, sequenced and cloned into pJN105.

Bacterial two-hybrid analysis. Protein interactions were tested using the BacterioMatch II Two-Hybrid System (Agilent Technologies). Briefly, the overnight cultures of the test strains were diluted to equal cell density. Five ten-fold serial dilutions of each culture were made and 5 µl of each was spotted on non-selective and dual-selective plates containing antibiotics and IPTG. The dual-selective plates had 5 mM 3-AT and 10 µg/ml streptomycin to test the strength

of the protein interactions. The negative control strain harbored empty pBT and pTRG vectors, while the positive control strain harbored *lgf2*:pBT and *galII*:pTRG as supplied by the manufacturer. The pBT and pTRG constructs were made using standard cloning techniques. The pairwise interactions tested included ParP-ParP, ParC-ParC, ParP-DipA, ParC-DipA, ParP-CheA, ParP-CheW, ParC- $PA2867_{161\text{-}490}$, and ParP- $PA2867_{161\text{-}490}$. PA2867 is a transmembrane receptor/MCP, and so a truncated version ($PA2867_{161\text{-}490}$ or tPA2867) containing only the C-terminal cytoplasmic portion was used.

SDS-PAGE and western blot. Whole cell lysates were prepared from mid-late log (OD_{600} 0.5-1) liquid cultures (37°C, with aeration). The cells were harvested and suspended in 2X SDS loading buffer, and loading was normalized based on OD_{600}. Whole cell lysates were separated by SDS-PAGE, and stained using Coomassie brilliant blue G-250 - perchloric acid solution [37]. The primary antibodies were α-His (1:3000), α-mCherry (1:1000) and α-GFP (1:1000). Secondary antibodies (1:10,000) conjugated to peroxidase allowed detection of signal using the SuperSignal West Femto Maximum Sensitivity Substrate kit. Western blots were visualized and imaged using a Fotodyne FOTO/Analyst FX system.

Swimming assay. Fresh *P. aeruginosa* colonies were stab inoculated into swimming media (1% tryptone, 0.5% NaCl and 0.3% agar) with antibiotics as appropriate. Following incubation at 30°C for 18 hours, the diameter of the swimming zones were measured. For each assay, 12 biological replicates were performed. ANOVA calculations were followed by the Tukey HSD post-hoc test using the R Console program (Version 3.2.3).

Fluorescence microscopy. Overnight cultures of *P. aeruginosa* were sub-cultured in LB broth with antibiotics as appropriate, and grown for three hours (with aeration at 37°C), resulting in cultures in mid-late log phase (OD_{600} 0.5 - 1). 5 µl of culture was spotted onto a polylysine-

355 treated coverslip (Fisherbrand 25CIR-1D) for observation using a Nikon Eclipse 90*i* microscope
356 with a Hamamatsu digital camera C11440 (ORCA-Flash 4.0) and a Nikon Intensilight C-GHFI
357 halogen lamp. Images were captured under DIC, Yfp, and Cfp filters, as appropriate. For
358 quantitation of localization patterns, between 248 and 300 cells were scored for foci formation
359 and localization. Foci were labeled as being polar if they fell within the curvature of the poles or
360 non-polar if they did not.

361 **Protein alignment.** Clustal Omega multiple sequence alignment was used for comparing the
362 amino acid sequences of multiple proteins [38].

363

364 **Acknowldegements:** The authors thank Zachary Zawada and Ashton Novy for their
365 contributions. We also thank Samuel Miller for indicated plasmid. The University of Washington
366 *Pseudomonas aeruginosa* transposon mutant collection is supported by NIH P30 DK089507.

367

368

369 1. Ringgaard S, Schirner K, Davis B, Waldor M. A family of ParA-like ATPAses promotes
370 cell pole maturation by facilitating polar localization of chemotaxis proteins. Genes and
371 Development. 2011;25:1544-55. doi: 10.1101/gad.2061811. PMCID: PMC3143943
372 2. Ringgaard S, Zepeda-Rivera M, Wu X, Schirner K, Davis B, Walder M. ParP prevents
373 dissociation of CheA from chemotactic signaling arrays and tethers them to a polar anchor.
374 Proceedings of the National Academy of Sciences USA. 2014;111:E255-64. doi:
375 10.1073/pnas.1315722111. PMCID: PMC3896188

3. Roberts M, Wadhams G, Hadfield K, Tickner S, Armitage J. ParA-like protein uses nonspecific chromosomal DNA binding to partition protein complexes. Proceedings of the National Academy of Sciences USA. 2012;109:6698-703. doi: 10.1073/pnas.1114000109. PMCID: PMC3340030

4. Treuner-Lange A, Søgaard-Andersen L. Regulation of cell polarity in bacteria. The Journal of Cell Biology. 2014;206(1):7-17. doi: 10.1083/jcb.201403136.

5. Heering J, Ringgaard S. Differential Localization of Chemotactic Signaling Arrays during the Lifecycle of Vibrio parahaemolyticus. Front Microbiol. 2016;7:1767. doi: 10.3389/fmicb.2016.01767. PMCID: PMC5090175.

6. Wadhams G, Martin A, Warren A, Armitage J. Requirements for chemotaxis protein localization in *Rhodobacter sphaeroides*. Molecular Microbiology. 2005;48:895-902. doi: 10.1111/j.1365-2958.2005.04880.x.

7. Sarkar MK, Paul K, Blair D. Chemotaxis signaling protein CheY binds to the rotor protein FliN to control the direction of flagellar rotation in Escherichia coli. Proceedings of the National Academy of Sciences. 2010;107(20):9370-5. doi: 10.1073/pnas.1000935107.

8. O'Connor JR, Kuwada NJ, Huangyutitham V, Wiggins PA, Harwood CS. Surface sensing and lateral subcellular localization of WspA, the receptor in a chemosensory-like system leading to c-di-GMP production. Mol Microbiol. 2012;86(3):720-9. doi: 10.1111/mmi.12013. PMCID: PMC3501340.

9. Ringgaard S, Yang W, Alvarado A, Schirner K, Briegel A. Chemotaxis arrays in Vibrio species and their intracellular positioning by the ParC/ParP system. Journal of Bacteriology. 2018. Epub 12 March 2018. doi: 10.1128/JB.00793-17.

398 10. Diaz MH, Hauser AR. Pseudomonas aeruginosa cytotoxin ExoU is injected into
399 phagocytic cells during acute pneumonia. Infect Immun. 2010;78(4):1447-56. doi:
400 10.1128/IAI.01134-09. PMCID: PMC2849415.
401 11. Fulcher N, Holliday P, Klem E, Cann M, Wolfgang M. The Pseudomonas aeruginosa
402 Chp chemosensory system regulates intracellular cAMP by levels modulating adenylate cyclase
403 activity. Molecular Microbiology. 2010;76:889-904. doi: 10.1111/j.1365-2958.2010.07135.x.
404 PMCID: PMC2906755.
405 12. Masduki A, Nakamura J, Ohga T, Umezaki R, Kato J, Ohtake H. Isolation and
406 characterization of chemotaxis mutants and genes of Pseudomonas aeruginosa. J Bacteriol.
407 1995;177(4):948-52. PMCID: PMC176688.
408 13. Kato J, Nakamura T, Kuroda A, Ohtake H. Cloning and characterization of chemotaxis
409 genes in *Pseudomonas aeruginosa*. Biosci Biotechnol Biochem. 1999;63:155-61. doi:
410 10.1271/bbb.63.155.
411 14. Cowles K, Moser T, Siryaporn A, Nyakudarika N, Dixon W, Turner J, et al. The putative
412 Poc complex controls two distinct *Pseudomonas aeruginosa* polar motility mechanisms.
413 Molecular Microbiology. 2013;90:923-38. doi: 10.1111/mmi.12403. PMCID: PMC4666538
414 15. Pandza S, Baetens M, Park CH, Au T, Keyhan M, Matin A. The G-protein FlhF has a
415 role in polar flagellar placement and general stress response induction in Pseudomonas putida.
416 Mol Microbiol. 2000;36(2):414-23.
417 16. Kulasekara BR, Kamischke C, Kulasekara HD, Christen M, Wiggins PA, Miller SI. c-di-
418 GMP heterogeneity is generated by the chemotaxis machinery to regulate flagellar motility.
419 Elife. 2013;2:e01402. doi: 10.7554/eLife.01402. PMCID: PMC3861689.

17. Romling U, Galperin MY, Gomelsky M. Cyclic di-GMP: the first 25 years of a universal bacterial second messenger. Microbiol Mol Biol Rev. 2013;77(1):1-52. doi: 10.1128/MMBR.00043-12. PMCID: PMC3591986.

18. Roy A, Petrova O, Sauer K. The phosphodiesterase DipA (PA5017) is essential for *Pseudomonas aeruginosa* biofilm dispersion. Journal of Bacteriology. 2012 194:2904-15. doi: 10.1128/JB.05346-11. PMCID: PMC3370607

19. Petrova OE, Sauer K. PAS domain residues and prosthetic group involved in BdlA-dependent dispersion response by Pseudomonas aeruginosa biofilms. J Bacteriol. 2012;194(21):5817-28. doi: 10.1128/JB.00780-12. PMCID: PMC3486124.

20. Basu Roy A, Sauer K. Diguanylate cyclase NicD-based signalling mechanism of nutrient-induced dispersion by Pseudomonas aeruginosa. Molecular Microbiology. 2014;94(4):771-93. doi: 10.1111/mmi.12802.

21. Li Y, Xia H, Bai F, Xu H, Yang L, Yao H, et al. Identification of a new gene PA5017 involved in flagella-mediated motility, chemotaxis and biofilm formation in Pseudomonas aeruginosa. FEMS Microbiol Lett. 2007;272(2):188-95. doi: 10.1111/j.1574-6968.2007.00753.x.

22. Guvener Z, Tifrea D, Harwood C. Two different *Pseudomonas aeruginosa* chemosensory signal transduction complexes localize to cell poles and remould in stationary phase. Molecular Microbiology. 2006;61:106-18. doi: 10.1111/j.1365-2958.2006.05218.x.

23. Briegel A, Wong ML, Hodges HL, Oikonomou CM, Piasta KN, Harris MJ, et al. New insights into bacterial chemoreceptor array structure and assembly from electron cryotomography. Biochemistry. 2014;53(10):1575-85. doi: 10.1021/bi5000614. PMCID: PMC3985956.

442 24. Dmowski M, Jagura-Burdzy G. Mapping of the interactions between partition proteins
443 Delta and Omega of plasmid pSM19035 from Streptococcus pyogenes. Microbiology.
444 2011;157(Pt 4):1009-20. doi: 10.1099/mic.0.045369-0.
445 25. Saaki TNV, Strahl H, Hamoen LW. Membrane curvature and the Tol-Pal complex
446 determine polar localization of the chemoreceptor Tar in E. coli. J Bacteriol. 2018. doi:
447 10.1128/JB.00658-17.
448 26. Greenfield D, McEvoy A, Shroff H, Crooks G, Wingreen N, Betzig E, et al. Self-
449 organization of the *Escherichia coli* chemotaxis network imaged with super-resolution light
450 microscopy. PLos Biology. 2009;7:e1000137. doi: 10.1371/journal.pbio.1000137. PMCID:
451 PMC2691949
452 27. Thiem S, Sourjik V. Stochastic assembly of chemoreceptor clusters in Escherichia coli.
453 Mol Microbiol. 2008;68(5):1228-36. doi: 10.1111/j.1365-2958.2008.06227.x.
454 28. Strahl H, Ronneau S, Gonzalez BS, Klutsch D, Schaffner-Barbero C, Hamoen LW.
455 Transmembrane protein sorting driven by membrane curvature. Nat Commun. 2015;6:8728. doi:
456 10.1038/ncomms9728. PMCID: PMC4632190.
457 29. Neeli-Venkata R, Startceva S, Annila T, Ribeiro AS. Polar Localization of the Serine
458 Chemoreceptor of Escherichia coli Is Nucleoid Exclusion-Dependent. Biophys J.
459 2016;111(11):2512-22. doi: 10.1016/j.bpj.2016.10.024. PMCID: PMC5153539.
460 30. Murray TS, Kazmierczak BI. FlhF is required for swimming and swarming in
461 Pseudomonas aeruginosa. J Bacteriol. 2006;188(19):6995-7004. doi: 10.1128/JB.00790-06.
462 PMCID: PMC1595508.
463 31. Sourjik V, Armitage JP. Spatial organization in bacterial chemotaxis. EMBO J.
464 2010;29(16):2724-33. doi: 10.1038/emboj.2010.178. PMCID: PMC2924652.

32. Cardozo MJ, Massazza DA, Parkinson JS, Studdert CA. Disruption of chemoreceptor signalling arrays by high levels of CheW, the receptor-kinase coupling protein. Mol Microbiol. 2010;75(5):1171-81. doi: 10.1111/j.1365-2958.2009.07032.x. PMCID: PMC5699227.

33. Hoang TT, Karkhoff-Schweizer RR, Kutchma AJ, Schweizer HP. A broad-host-range Flp-FRT recombination system for site-specific excision of chromosomally-located DNA sequences: application for isolation of unmarked Pseudomonas aeruginosa mutants. Gene. 1998;212(1):77-86.

34. Jansari VH, Potharla VY, Riddell GT, Bardy SL. Twitching motility and cAMP levels: signal transduction through a single methyl-accepting chemotaxis protein. FEMS Microbiol Lett. 2016;363(12). doi: 10.1093/femsle/fnw119.

35. Horton RM, Cai ZL, Ho SN, Pease LR. Gene splicing by overlap extension: tailor-made genes using the polymerase chain reaction. Biotechniques. 1990;8(5):528-35.

36. Newman JR, Fuqua C. Broad-host-range expression vectors that carry the L-arabinose-inducible Escherichia coli araBAD promoter and the araC regulator. Gene. 1999;227(2):197-203.

37. Faguy DM, Bayley DP, Kostyukova AS, Thomas NA, Jarrell KF. Isolation and characterization of flagella and flagellin proteins from the Thermoacidophilic archaea *Thermoplasma volcanium* and *Sulfolobus shibatae*. Journal of Bacteriology. 1996;178(3):902-5.

38. Sievers F, Wilm A, Dineen D, Gibson TJ, Karplus K, Li W, et al. Fast, scalable generation of high-quality protein multiple sequence alignments using Clustal Omega. Mol Syst Biol. 2011;7:539. doi: 10.1038/msb.2011.75. PMCID: PMC3261699.

39. Simon R, Priefer U, Pühler A. A Broad Host Range Mobilization System for In Vivo Genetic Engineering: Transposon Mutagenesis in Gram Negative Bacteria. Bio/Technology. 1983;1:784. doi: 10.1038/nbt1183-784.

Figure Legends

Fig. 1. Par-like proteins encoded within chemotaxis gene cluster I (*che I*) are required for optimal swimming motility. A) *che I* gene cluster of *P. aeruginosa* (drawn to scale). B) Swimming motility assay of wild type (PAO1) and indicated *P. aeruginosa* strains. Δ*che I* strain lacks the chemotaxis genes *cheY, cheZ, cheA, cheB,* and *cheW.* The average swimming diameter measurements are shown and error bars denote the standard error of the mean. Matching letters indicate statistically significant differences, $p<0.001$. (V) indicates empty vector (pJN105).

Fig. 2. The Par-like proteins affect chemotaxis protein localization. A) Representative images of CheA:mTq foci formation in wild type (PAO1) and indicated *P. aeruginosa* strains. B) Quantitation of CheA:mTq foci localization in the indicated *P. aeruginosa* strains. 248 cells per strain were counted. C) CheA:mTq expression levels as determined through western blotting. D) Expression of CheA:mTq supports swimming motility. Average swimming diameter is shown and error bars denote the standard error of the mean. All values were significantly different from wild type, $p<0.001$.

Fig 3. DipA interacts directly with ParP, as demonstrated by a bacterial two-hybrid assay. 5 µl of a 10-fold dilution series are spotted from left to right. Cultures on the non-selective media function as a loading control, while dual-selective media reveals the strength of the protein-protein interactions. Strong interactions have growth to the right-most spot, as indicated by the positive control *lgf2* and *galII.*

Fig. 4. Deletion of DipA results in a similar reduction of swimming motility as seen in Δ*parP.*

511 (A) Swimming motility assay of indicated *P. aeruginosa* strains. The averaged swimming
512 diameters are shown and error bars denote standard error of the mean. Matching letters indicate
513 statistically significant differences, p>0.001. (B)Western blot showing expression of His-DipA.
514
515 **Fig. 5.** DipA is not required for CheA foci formation or localization. (A) Representative images
516 of CheA-mTq foci formation in wild type and mutant *P. aeruginosa* strains. (B) Quantitation of
517 CheA-mTq foci formation and localization in the indicated *P. aeruginosa* strains. 300 cells were
518 counted per strain. (C) Western blot showing CheA-mTq levels.
519
520 **Fig. 6.** DipA and CheA influence ParP foci formation. (A) Representative images of Yfp-ParP
521 foci formation in wild type and mutant *P. aeruginosa* strains. (B) Western blot showing Yfp-
522 ParP levels in the indicated strains. (C) Quantitation of Yfp-ParP foci formation and localization
523 patterns in the indicated *P. aeruginosa* strains. 300 cells were counted per strain.
524
525 **Fig. 7.** DipA foci formation is influenced by ParP and dependent on CheA. (A) Representative
526 images of DipA-Yfp foci formation in wild type and mutant *P. aeruginosa* strains. (B) Western
527 blot showing DipA-Yfp levels in the indicated strains. (C) DipA-Yfp foci formation and
528 localization patterns in the indicated *P. aeruginosa* strains. 300 cells were counted per strain.
529
530 **Fig. 8**. Model showing B2H interactions linking the Par-like proteins with the chemotaxis and
531 biofilm dispersion systems of *P. aeruginosa*. Black arrows indicate direct protein-protein
532 interactions, with thicker arrows being a stronger interaction. The green dashed arrow points to
533 the different roles that DipA has in regards to biofilm dispersion and chemotaxis. The red arrow

534 pointing down indicates a decrease in c-di-GMP levels. The blue arrow represents a nutrient cue

535 that is sensed by NicD.

536

537

538 **Supplemental Table 1: Plasmids used in this study**

Plasmid	Description	Source
Δ*cheA*:pEX18Tc	DNA fusion product for deletion of *cheA* cloned into the EcoRI (5') and BamHI (3') sites of pEX18Tc	This study
Δ*cheW*:pEX18Tc	DNA fusion product for deletion of *cheW* cloned into the EcoRI (5') and BamHI (3') sites of pEX18Tc	This study
Δ*dipA*:pEX18Tc	DNA fusion product for deletion of *dipA* cloned into the EcoRI (5') and SacI (3') sites of pEX18Tc	This study
Δ*parC*:pEX18Tc	DNA fusion product for deletion of *parC* cloned into the EcoRI (5') and BamHI (3') sites of pEX18Tc	This study
Δ*parP*:pEX18Gm	DNA fusion product for deletion of *parP* cloned into the EcoRI (5') and HindIII (3') sites of pEX18Gm	This study
cheA-mTq:pEX18Gm	DNA fusion product for insertion of *cheA-mTurquoise* at the native chromosomal site, cloned into pEX18Gm	[16]
dipA-yfp:pUC18T-mini-TN7T-Gm	Plasmid template for amplifying *dipA-yfp*	[16]
pJN105	Broad host range vector. pBBR-1 MCS5 AraC-pBAD derivative	[36]
his-*cheW*:pJN105	his-*cheW* cloned into the EcoRI (5') and SacI (3') sites of pJN105	This study
his-*dipA*:pJN105	his-*dipA* cloned into the EcoRI (5') and XmaI (3') sites of pJN105	This study
parC:pJN105	*parC* cloned into the EcoRI (5') and XbaI (3') sites of pJN105	This study
parC-his:pJN105	*parC*-his cloned into the EcoRI (5') and XbaI (3') sites of pJN105	This study
his-*parP*:pJN105	his-*parP* cloned into the EcoRI (5') and SacI (3') sites of pJN105	This study
dipA-yfp:pJN105	*dipA-yfp* amplified from *dipA-yfp*:pUC18T-mini-TN7T-Gm and cloned into the EcoRI (5') and XbaI (3') sites of pJN105	This study
yfp-parP:pJN105	DNA fusion product *yfp-parP* cloned into the EcoRI (5') and SacI (3') sites of pJN105	This study

539

pBT	Expression vector used for Bacterial Two-Hybrid	Agilent Technologies
pTRG	Expression vector used for Bacterial Two-Hybrid	Agilent Technologies
cheA:pTRG	*cheA* cloned into the BamHI (5') and EcoRI (3') sites of pTRG	This study
dipA:pBT	*dipA* cloned into the NotI (5') and EcoRI (3') sites of pBT	This study
*mcpS:*pTRG	*mcpS* cloned into the XhoI (5') and NotI (3') sites of pTRG	This study
parC:pBT	*parC* cloned into the NotI (5') and EcoRI (3') sites of pBT	This study
parC:pTRG	*parC* cloned into the NotI (5') and EcoRI (3') sites of pTRG	This study
parP:pBT	*parP* cloned into the NotI (5') and EcoRI (3') sites of pBT	This study
tPA2867:pTRG	tPA2867 cloned into the EcoRI (5') and XhoI (3') sites of pTRG	This study

547 **Supplemental Table 2: Strains used in this study**

Strain	Description	Source
E. coli BacterioMatch II Two-Hybrid System Reporter Strain	*Δ(mcrA)183 Δ(mcrCB-hsdSMR-mrr)173 endA1 hisB supE44 thi-1 recA1 gyrA96 relA1 lac [F´ lacI^q HIS3 aadA Kan^r]*	Agilent Technologies
E. coli XL-1 Blue MRF' kan^r	*Δ(mcrA)183 Δ(mcrCB-hsdSMR-mrr)173 endA1 supE44 thi-1 recA1 gyrA96 relA1 lac [F´ proAB lacI^q ZΔM15 Tn5 (Kan^r)]*	Agilent Technologies
E. coli XL-1 Blue MRF' tet^r	*recA1 endA1 gyrA96 thi-1 hsdR17 supE44 relA1 lac [F´ proAB lacI^q ZΔM15 Tn10 (Tet^r)]*	Agilent Technologies
E. coli S17-1	*Tp^R Sm^R recA thi pro hsdR$^-$ M+ RP4 2-Tc::Mu-Km::Tn7 λpir*	[39]
E. coli NEB5α	*fhuA2 Δ(argF-lacZ)U169 phoA glnV44 Φ80 Δ(lacZ)M15 gyrA96 recA1 relA1 endA1 thi-1 hsdR17*	New England Biolabs
PAO1	*P. aeruginosa* PAO1 (Iglewski strain)	Carrie Harwood
PAO1 *cheA-mTq*	*cheA-mTq* at the native chromosomal site in PAO1	This study
PAO1 Δ*cheA*	In-frame deletion of PA1458 (*cheA*) in PAO1	This study
PAO1 Δ*cheW*	(+9) deletion of PA1464 (*cheW*) in PAO1	This study
PAO1 Δ*che I*	In-frame deletions of PA1456 (*cheY*), PA1457 (*cheZ*), PA1458 (*cheA*), PA1459 (*cheB*), and PA1464 (*cheW*) in PAO1	Carrie Harwood
PAO1 Δ*dipA*	(+9) deletion of PA5017 (*dipA*) in PAO1	This study
PAO1 *fliC::tn*	Transposon (lacZhah) in PA1092 (*fliC*) in PAO1. Inserted at base 820 of 1467	University of Washington PAO1 transposon mutant collection
PAO1 Δ*parC*	In-Frame deletion of PA1462 (*parC*) in PAO1	This study
PAO1 Δ*parP*	(+9) deletion of PA1463 (*parP*) in PAO1	This study

548

549

550

551 **Supplemental Table 3: Primers used in this study**

Primer name	**Sequence (5' to 3')**
Gene deletion	
cheA(Up)-for	GCGACGAATTCGAATCGACCCTG
cheA(Up)-rev	CGGAAACCCATACGCGGCGTCGGCTGCTCCCAGAGACGTG
cheA(Dn)-for	CACGTCTCTGGGAGCAGCCGACGCCGCGTATGGGTTTCCG
cheA(Dn)-rev	GAGGATCCCTGCTTGAGCAGGCGCGCAC
cheW(Up)-for	GCGACGAATTCCAGGCGCATTCAAGCCGCAC
cheW(Up)-rev	GTAGAACGCATCAGATGCTTTTGCTCATTCCCCTAACC
cheW(Dn)-for	GGTTAGGGGAATGAGCAAAAGCATCTGATGCGTTCTAC
cheW(Dn)-rev	GAGGATCCCTGGCCATTCTCCAGCACC
dipA(Up)-for	ATAGGAATTCATCACCGACATGGAAGCCTTC
dipA(Up)-rev	GCCTGGGCGATCAGTGCAGACTTTTCATGCGAGGCTGATTCC
dipA(Dn)-for	GAATCAGCCTCGCATGAAAAGTCTGCACTGATCGCCCAGGC
dipA(Dn)-rev	GAAAGAGCTCGCGCCAGCTCAAGCGTTTC
parC(Up)-for	GAGAATTCCACGAACGCTGGCTGGTTTC
parC(Up)-rev	CGGCGACCGGCGCGCCATGCTCTACTCTTCCTGGCATG
parC(Dn)-for	CATGCCAGGAAGAGTAGAGCATGGCGCGCCGGTCGCCG
parC(Dn)-rev	GAGGATCCCTATCAATGGTCGCCGTGCAG
parP(Up)-for	GAGATGAATTCGTCGCCTTCGCCATGAGCG
parP(Up)-rev	GAAGCTGTCTATCAATGGTCGGCGCTCATGTGGGTATTCC
parP(Dn)-for	GGAATACCCACATGAGCGCCGACCATTGATAGACAGCTTCCG
parP(Dn)-rev	GAGATAAGCTTGAAGTGGCGAGCCGCCTG
Bacterial two-hybrid	
cheA-pTRG-for	GCGGATCCATGAGCTTCGACGCCGATGA
cheA-pTRG-rev	CGGAATTCAGTCTACGCGGCACGCATTG
dipA-pBT/TRG-for	AGACGCGGCCGCTATGAAAAGTCATCCCGATGCCGCC
dipA-pBT/TRG-rev	ATTGGAATTCTCAGTGCAGGGTGCGGCAG
parC-pBT/TRG-for	AGCGGCCGCTATGAAAGTCTGGGCAGTCG
parC-pBT/TRG-rev	ATACGAATTCTCAGGCCACCCGGGTGGC
parP-pBT/TRG-for	AGCGGCCGCTATGAGCGCCGCCACCGCC
parP-pBT/TRG-rev	ATACGAATTCTCAATGGTCGCCGTGCAGG
tPA2867-pTRG-for	ATACGAATTCTTTTCATCCTCACCCACCTGC
PA2867-pBT/TRG-rev	ATACCTCGAGTCAGAGGCGTAGCTGGCCG

552

553

554

555

556

Complementation	
his-*cheW*-for	GTTAAGAATTCATGCACCACCATCACCACCATAGCAAAGCCACCGCGCAAAGC
cheW-rev	CTAGAGCTCTCAGATGCTGCCCAGCTCCG
his-*dipA*-for	TTCAGAATTCATGCACCACCATCACCACCATAAAAGTCATCCCGATGCCGCC
dipA-rev	TGCCCGGGTCAGTGCAGGGTGCGGCAG
parC-for	GTTAAGAATTCATGAAAGTCTGGGCAGTCGC
parC-rev	CTATCTAGAACTCCGGTGCGGCTTGAATG
parC-his-rev	CTATCTAGATCAATGGTGGTGATGGTGGTGGGCCACCCGGGTGGCCGGC
his-*parP*-for	GTTAAGAATTCATGCACCACCATCACCACCATAGCGCCGCCACCGCCACCC
parP-rev	CTAGAGCTCTCAATGGTCGCCGTGCAGG
Fluorescence microscopy	
dipA(*yfp*)-for	TTCAGAATTCATGAAAAGTCATCCCGATGCCG
yfp(*dipA*)-rev	CTATCTAGATTACTTGTACAGCTCGTCCATG
yfp(*parP*)-for	ATTGGAATTCATGGTGAGCAAGGGCGAGGAG
yfp(*parP*)-rev	GTGGCGGTGGCGGCGCTCATCTTGTACAGCTCGTCCATGCC
parP(*yfpA*)-Dn-for	CATGGACGAGCTGTACAAGATGAGCGCCGCCACCGCCAC
parP(*yfpA*)-Dn-rev	GAAGAGCTCTCAATGGTCGCCGTGCAGG

557

558

559

560

561

562

563

564

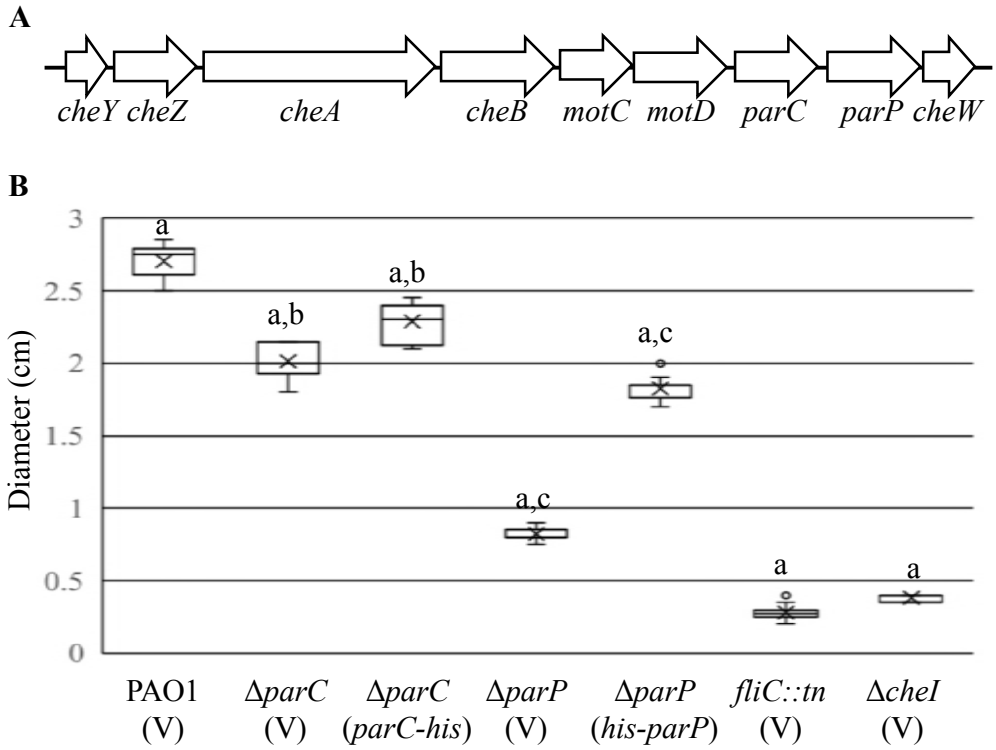

Fig. 1. Par-like proteins encoded within chemotaxis gene cluster I (*che I*) are required for optimal swimming motility. A) *che I* gene cluster of *P. aeruginosa* (drawn to scale). B) Swimming motility assay of wild type (PAO1) and indicated *P. aeruginosa* strains. Δ*che I* strain lacks the chemotaxis genes *cheY*, *cheZ*, *cheA*, *cheB*, and *cheW*. The average swimming diameter measurements are shown and error bars denote the standard error of the mean. Matching letters indicate statistically significant differences, $p<0.001$. (V) indicates empty vector (pJN105).

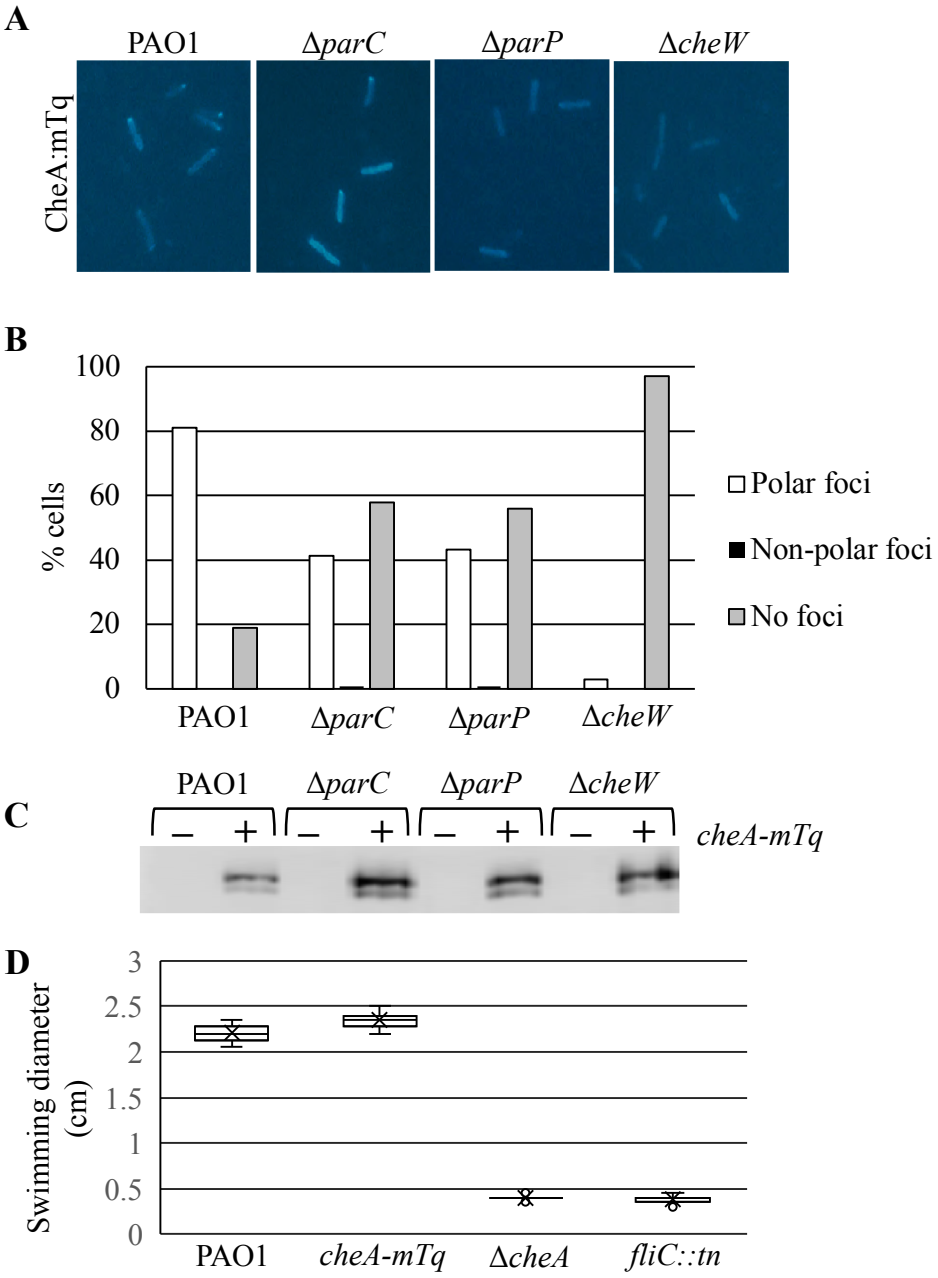

Fig. 2. The Par-like proteins affect chemotaxis protein localization. A) Representative images of CheA:mTq foci formation in wild type (PAO1) and indicated *P. aeruginosa* strains. B) Quantitation of CheA:mTq foci localization in the indicated *P. aeruginosa* strains. 248 cells per strain were counted. C) CheA:mTq expression levels as determined through western blotting. D) Expression of CheA:mTq supports swimming motility. Average swimming diameter is shown and error bars denote the standard error of the mean. All values were significantly different from wild type, $p<0.001$.

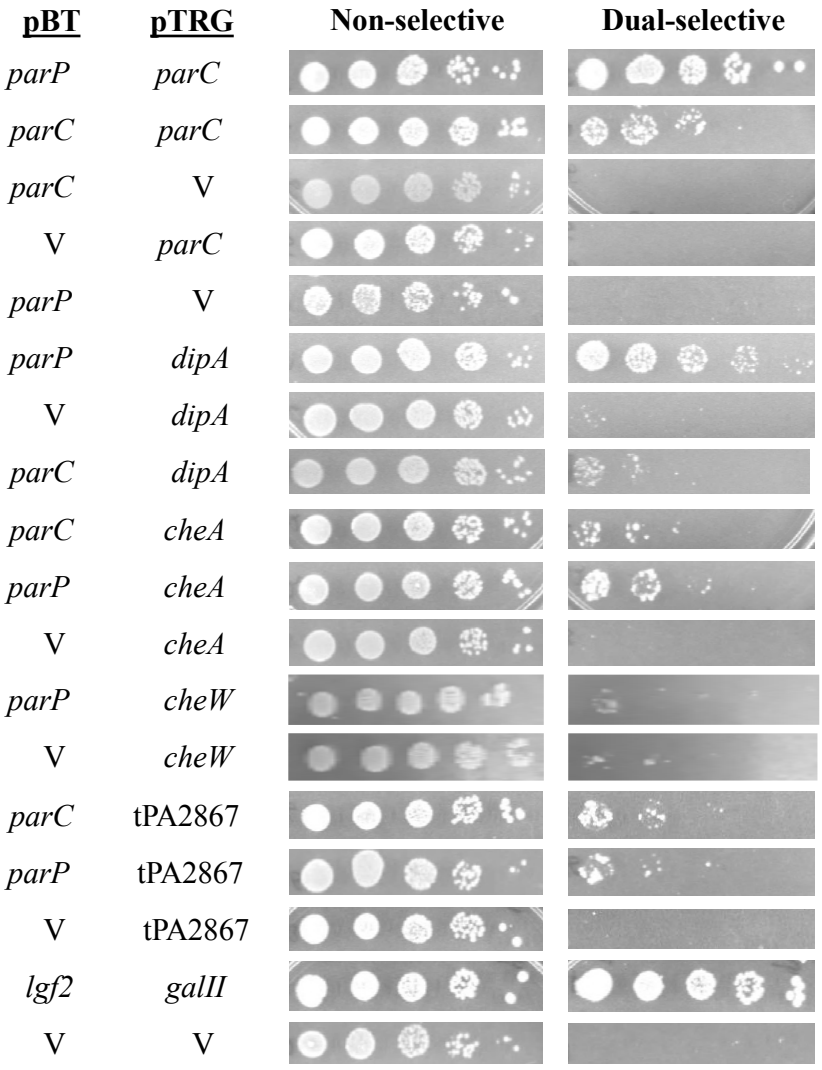

Fig 3. DipA interacts directly with ParP, as demonstrated by a bacterial two-hybrid assay. 5 µl of a 10-fold dilution series are spotted from left to right. Cultures on the non-selective media function as a loading control, while dual-selective media reveals the strength of the protein-protein interactions. Strong interactions have growth to the right-most spot, as indicated by the positive control *lgf2* and *galII*.

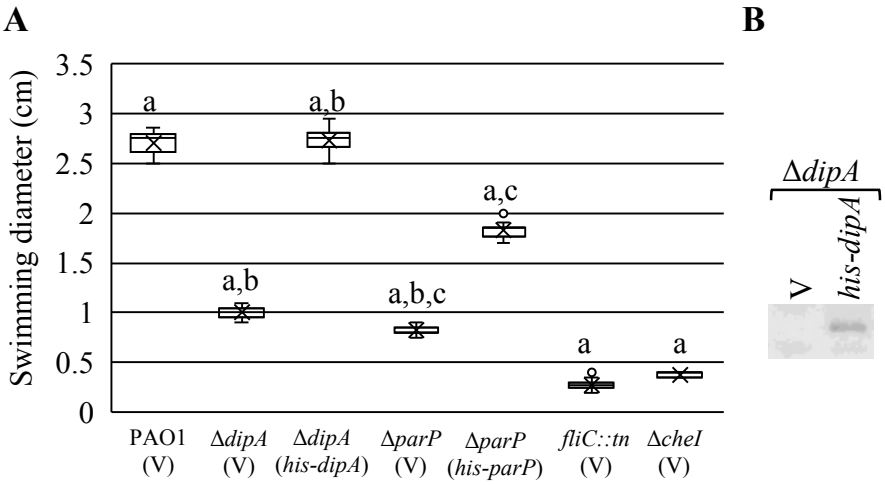

Fig. 4. Deletion of DipA results in a similar reduction of swimming motility as seen in Δ*parP*. (A) Swimming motility assay of indicated *P. aeruginosa* strains. The averaged swimming diameters are shown and error bars denote standard error of the mean. Matching letters indicate statistically significant differences, p>0.001. (B)Western blot showing expression of His-DipA.

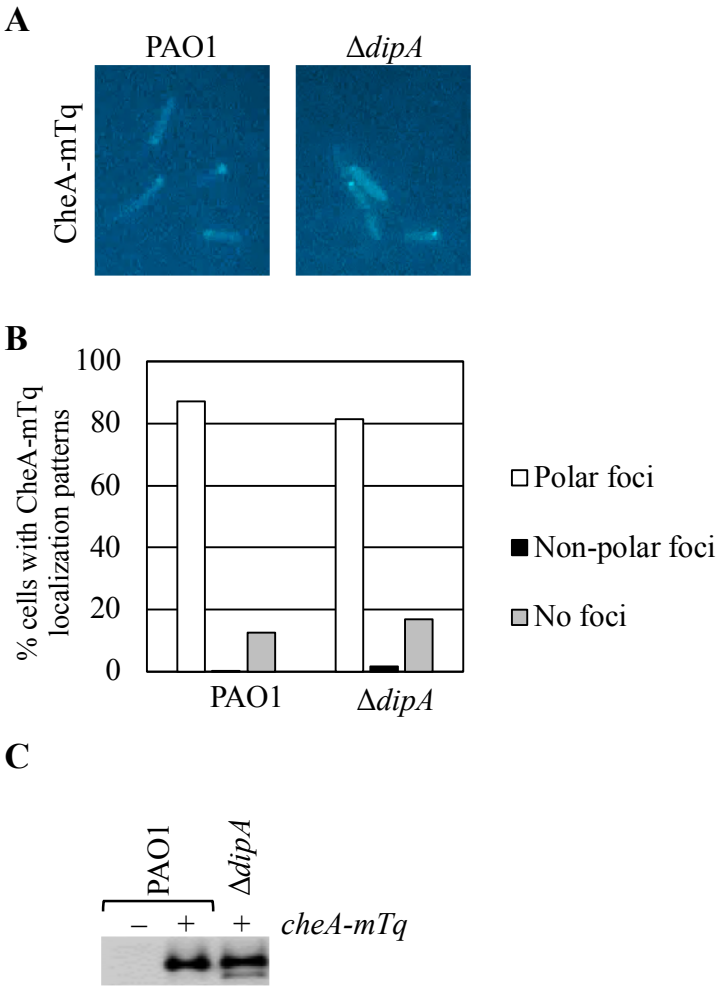

Fig. 5. DipA is not required for CheA foci formation or localization. (A) Representative images of CheA-mTq foci formation in wild type and mutant *P. aeruginosa* strains. (B) Quantitation of CheA-mTq foci formation and localization in the indicated *P. aeruginosa* strains. 300 cells were counted per strain. (C) Western blot showing CheA-mTq levels.

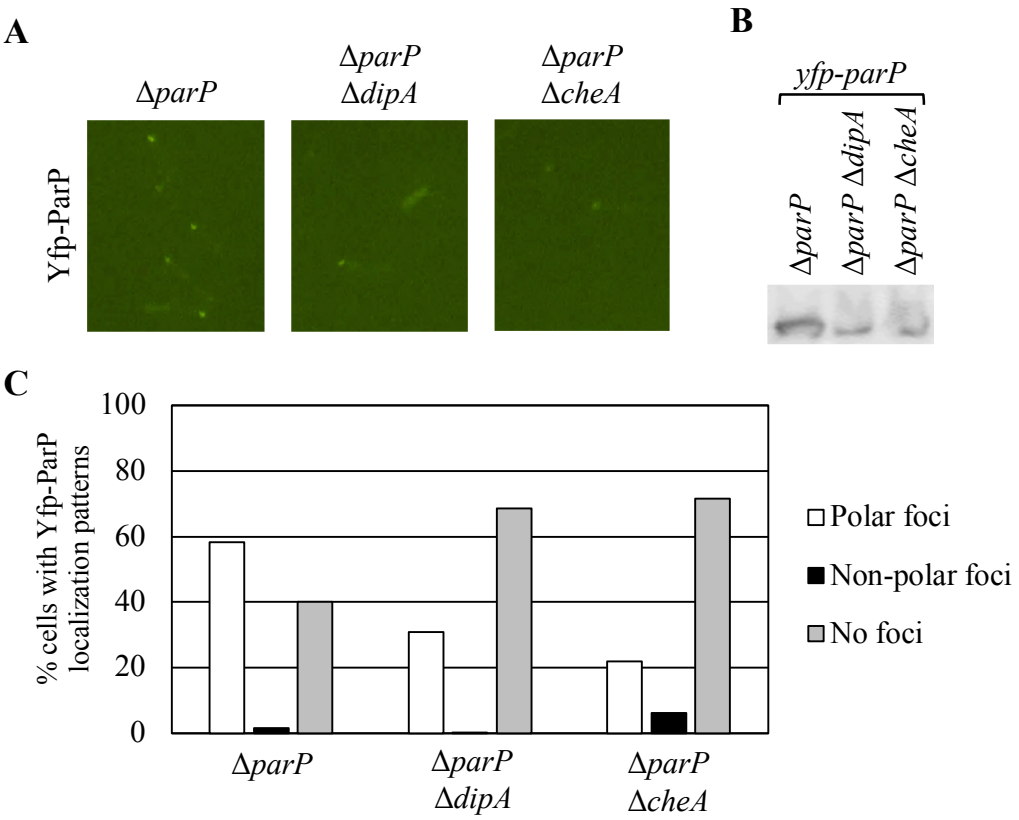

Fig. 6. DipA and CheA influence ParP foci formation. (A) Representative images of Yfp-ParP foci formation in wild type and mutant *P. aeruginosa* strains. (B) Western blot showing Yfp-ParP levels in the indicated strains. (C) Quantitation of Yfp-ParP foci formation and localization patterns in the indicated *P. aeruginosa* strains. 300 cells were counted per strain.

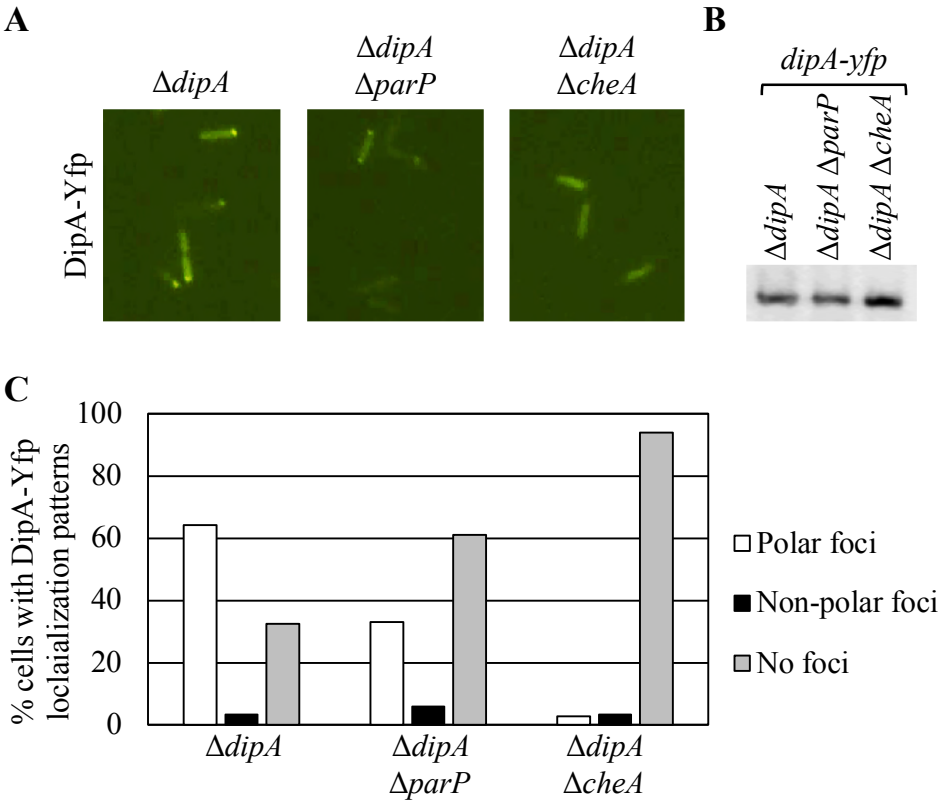

Fig. 7. DipA foci formation is influenced by ParP and dependent on CheA. (A) Representative images of DipA-Yfp foci formation in wild type and mutant *P. aeruginosa* strains. (B) Western blot showing DipA-Yfp levels in the indicated strains. (C) DipA-Yfp foci formation and localization patterns in the indicated *P. aeruginosa* strains. 300 cells were counted per strain.

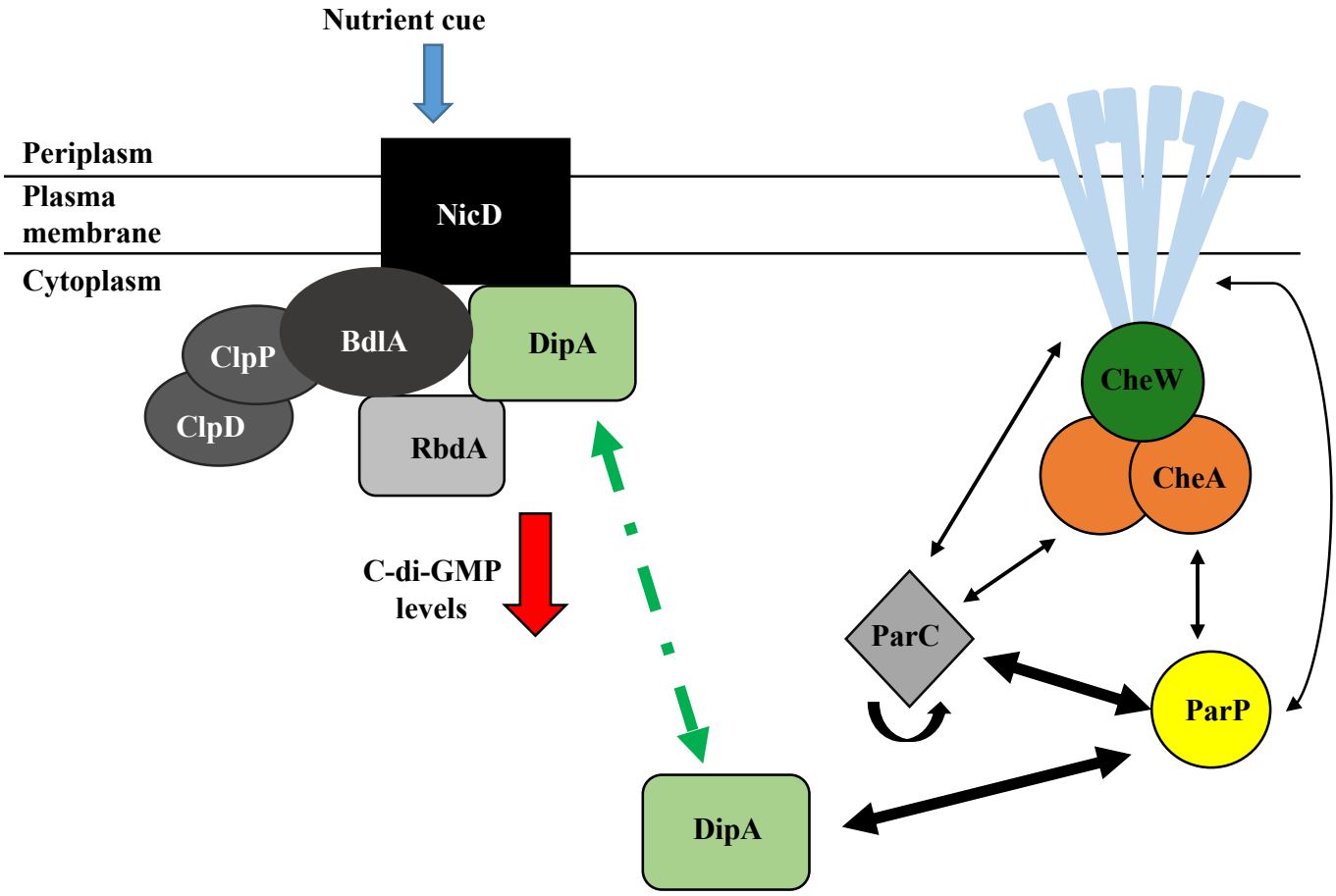

Fig. 8. Model showing B2H interactions linking the Par-like proteins with the chemotaxis and biofilm dispersion systems of *P. aeruginosa*. Black arrows indicate direct protein-protein interactions, with thicker arrows being a stronger interaction. The green dashed arrow points to the different roles that DipA has in regards to biofilm dispersion and chemotaxis. The red arrow pointing down indicates a decrease in c-di-GMP levels. The blue arrow represents a nutrient cue that is sensed by NicD.